

Nonparametric Quantile-Based Causal Discovery

Natasa Tagasovska ^{*} Thibault Vatter [†]
Valérie Chavez-Demoulin[‡]

May 17, 2022

Abstract

Distinguishing cause from effect using observational data is a challenging problem, especially in the bivariate case. Contemporary methods often assume an independence between the cause and the generating mechanism of the effect given the cause. From this postulate, they derive asymmetries to uncover causal relationships. Leveraging the same postulate, in this work, we propose a novel approach based on the link between Kolmogorov complexity and quantile scoring. We use a nonparametric conditional quantile estimator based on copulas to implement our procedure, thus avoiding restrictive assumptions about the joint distribution between cause and effect. In an extensive study on real and synthetic data, we show that quantile copula causal discovery (QCCD) compares favorably to state-of-the-art methods.

Keywords: causal discovery, quantile scoring, minimum description length, nonparametric, copula

1. Introduction

Motivated by the usefulness of causal inference in almost any field of science, an increasing body of research has contributed towards understanding the generative processes behind data. The aim is the elevation of learning models towards more powerful interpretations: from correlations and dependencies towards *causation* (Pearl, 2009, Pearl et al., 2016, Lopez-Paz, 2016).

^{*}Department of Information Systems, HEC Lausanne. E-mail: natasa.tagasovska@unil.ch

[†]Department of Statistics. Columbia University. E-mail: tv2233@columbia.edu

[‡]Department of Operations, HEC Lausanne. E-mail: valerie.chavez@unil.ch

While the golden standard for causal discovery is randomized control trials (Fisher, 1936), experiments or interventions in a system are often prohibitively expensive, unethical, or, in many cases, impossible. In this context, an alternative is to use observational data to infer causal relationships (Maathuis and Nandy, 2016). This challenging task has been tackled by many, often relying on testing conditional independence and backed up by heuristics (Maathuis and Nandy, 2016, Spirtes and Zhang, 2016, Peters et al., 2017).

Borrowing from structural equations and graphical models, structural causal models (SCMs, Pearl et al., 2016, Peters et al., 2017) represent the causal structure of variables X_1, \dots, X_d using equations such as

$$X_c = f_c(X_{PA(c), \mathcal{G}}, E_c), \quad c \in \{1, \dots, d\},$$

where

- f_c is a causal mechanism linking the child/effect X_c to its parents/direct causes $X_{PA(c), \mathcal{G}}$,
- E_c is another variable independent of $X_{PA(c), \mathcal{G}}$,
- and \mathcal{G} is the directed graph obtained from drawing arrows from parents to their children.

Further complications arise when observing only two variables. In this case, one cannot distinguish between latent confounding ($X \leftarrow Z \rightarrow Y$) and direct causation ($X \rightarrow Y$ or $X \leftarrow Y$) without additional assumptions (Lopez-Paz et al., 2015). A possible solution to this open question is to impose certain model restrictions. For example, (non-)linear additive noise models, with $Y = f(X) + E_Y$, provide a foundation for establishing *identifiability* (Shimizu et al., 2006, Hoyer et al., 2009, Peters et al., 2011). An extension is the post nonlinear model (Zhang and Hyvärinen, 2009), $Y = g(f(X) + E_Y)$, with g being an invertible function. Another line of work avoids functional restrictions by relying on the *independence of cause and mechanism* postulate (Schölkopf et al., 2012, Peters et al., 2017):

Postulate 1 (Sgouritsa et al. 2015). *The marginal distribution of the cause and the conditional distribution of the effect, given the cause corresponding to independent mechanisms of nature, are independent (i.e., they contain no information about each other).*

Information Geometric Causal Inference (IGCI) (Janzing et al., 2012), one of the best-performing algorithms in a recent benchmarking study (Mooij et al., 2016), uses the postulate directly for causal discovery. Alternatively Mooij et al. (2010) and Janzing and Schölkopf (2010) reformulate the postulate through asymmetries in Kolmogorov complexities (Kolmogorov, 1963) between marginal and conditionals distributions. However, the halting problem (Turing, 1937, 1938) implies that the Kolmogorov complexity is not computable, and approximations or proxies have to be derived to make the concept practical. In this context, Mooij et al. (2010) proposes an approximation based on the minimum message

length (MML) principle using Bayesian priors, while other methods are based on reproducing kernel Hilbert space embedding such as EMD (Chen et al., 2014) or FT (Liu and Chan, 2017). A related line of work suggests using the minimum description length (MDL, Rissanen, 1978) principle as a proxy for Kolmogorov complexity: Budhathoki and Vreeken (2017) uses MDL for causal discovery on binary data, and Slope (Marx and Vreeken, 2017) implements local and global functional relations using MDL-based regression and is suitable for continuous data.

In this work, we build on a similar idea, using *quantile scoring* as a proxy for the Kolmogorov complexity through the MDL principle. To the best of our knowledge, quantiles have only been mentioned in a somewhat related context by Heinze-Deml et al. (2017), where quantile predictions are used to exploit the invariance of causal models across different environments. As opposed to Heinze-Deml et al. (2017), our method uses an asymmetry directly derived from the postulate, and therefore it does not require an additional variable for the environment.

To avoid the restrictive assumptions imposed by standard quantile regression techniques, we estimate conditional quantiles fully nonparametrically using *copulas*. Since the introduction of the pitfalls of correlations (Embrechts et al., 1999), there has been a growing body of literature on copula-based methodology and applications in the statistics community. In a nutshell, copulas make it possible to flexibly model the dependence structure between random variables while avoiding assumptions about the scales, functional forms, or other restrictions imposed when dealing with marginal distributions. More recently, copulas have made their way into machine learning research as well (Liu et al., 2009, Elidan, 2013, Lopez-Paz et al., 2013, Tran et al., 2015, Lopez-Paz, 2016, Chang et al., 2016). In the context of structure learning, copulas have been explored in the Gaussian copula setting (Harris and Drton, 2013, Cui et al., 2016) or with pair-copula constructions (Bauer and Czado, 2016, Pircalabelu et al., 2017, Müller and Czado, 2017). However, such approaches are not targeted at pairwise causal discovery.

To the best of our knowledge, we are the first to explore the idea of using conditional quantiles to distinguish cause from effect in bivariate observational data. Our main contributions are:

- a new method based on quantile scoring to determine the causal direction in bivariate datasets without restricting assumptions on the class of causal mechanisms,
- a theoretical analysis justifying its usage,
- *quantile copula causal discovery* (QCCD), an efficient algorithmic implementation,
- a comparative study to benchmark QCCD against state-of-the-art alternatives.

The rest of the paper is organized as follows. Section 2 introduces quantile scoring from a decision-theoretic perspective. Section 2.2 then builds upon the link between quantile scoring and Kolmogorov complexity to formulate the quantile-based causal decision rule. Section 2.4, Section 3.1, and Section 3.2 further

explain the proposed methodology and its implementation with nonparametric copulas. Section 4 presents a set of experiments on real and simulated datasets. We conclude in Section 5.

2. Nonparametric causal discovery using quantiles and copulas

In this section, we develop our quantile-based method for distinguishing between cause and effect from continuous and discrete observational data. We restrict ourselves to bivariate cases by considering pairs of univariate random variables. We further simplify the problem by assuming no confounding, no selection bias, and no feedback.

2.1. Quantile scoring

To introduce our score for quantile-based causal discovery, we first describe its statistical decision-theoretic roots and refer to Gneiting (2011) for more details. Let I be the range of potential outcomes (e.g., $I = \mathbb{R}$) and $Z \in I$ be a random variable (r.v.) with distribution $F \in \mathcal{F}$, where \mathcal{F} is a family of distributions taking values in I . In this context, a *scoring function* is then any map $S : I \times I \rightarrow [0, \infty)$, and an *optimal point forecast* under S is then a minimizer of the expected score $\hat{z} = \operatorname{argmin}_z \mathbb{E}_F [S(z, Z)]$. Let a *functional* T be any mapping $F \rightarrow T(F) \subseteq I$.

Definition 1 (Consistent scoring function). *A scoring function S is said to be consistent for T relative to \mathcal{F} if $\mathbb{E}_F [S(t, Z)] \leq \mathbb{E}_F [S(z, Z)]$ for all $F \in \mathcal{F}$, $t \in T(F)$, and $z \in I$. Furthermore, S is strictly consistent if it is consistent and equality implies that $z \in T(F)$.*

Example 1 (Mean and squared loss). For the functional $\mu = \mathbb{E}_F [Z]$ and scoring function $S(z_1, z_2) = (z_1 - z_2)^2$, μ is the optimal point forecast under S , and S is consistent for μ .

This example helps build an intuition about the links between functionals, optimal point forecasts, and consistent scoring functions. These relationships can be further formalized as follows:

Theorem 1 (Gneiting 2011). *For any $F \in \mathcal{F}$ and $T(F)$, $t \in T(F)$ is an optimal point forecast under S if and only if S is consistent for $T(F)$ relative to \mathcal{F} .*

In other words, there is a duality between point forecast optimality and consistency, or between making and evaluating point forecasts.

Example 2 (Quantile scoring). The τ -quantile is $\mu_\tau = F^{-1}(\tau) = \arg \inf_\mu \{\mu \mid F(\mu) = \tau\}$. If i is an increasing function (e.g., the identity $i(z) = z$) and \mathbb{I} is the indicator

function, then the scoring function $S_\tau(z_1, z_2) = (\mathbb{I}\{z_1 \geq z_2\} - \tau)(i(z_1) - i(z_2))$ is consistent for the τ -quantile (Gneiting, 2011).

Note that finding $\hat{\mu}_\tau = \operatorname{argmin}_{\mu_\tau} \mathbb{E}_F[S(\mu_\tau, Z)]$ for S as in Example 2 with $i(z) = z$ can be related to maximum likelihood estimation for asymmetric Laplace (AL) distributions¹, see Aue et al. (2014), Geraci and Bottai (2006), Yu et al. (2003). Essentially, if $Z - \mu_\tau$ follows an AL distribution, then $\hat{\mu}_\tau$ as above is also the maximizer of the likelihood $L(\mu_\tau) \propto \exp(-\sum_{i=1}^n S_\tau(\mu_\tau, Z_i))$.

Let F_X and $F_{Y|X}$ denote the marginal and conditional distributions, corresponding to X and $Y|X$. For $\tau \in [0, 1]$, the marginal and conditional *quantile scores* (QSs) of X and $Y|X$ are

$$\begin{aligned} S_X(\tau) &= \mathbb{E}[S_\tau(F_X^{-1}(\tau), X)] \\ S_{Y|X}(\tau) &= \mathbb{E}[S_\tau(F_{Y|X}^{-1}(X, \tau), Y)] \end{aligned}$$

where S is as in Example 2 using the identity $i(z) = z$, the inverses are with respect to τ , and $S_Y(\tau)$ and $S_{X|Y}(\tau)$ for Y and $X|Y$ can be defined similarly. In the next section, we link asymmetries between the quantile scores to asymmetries in Kolmogorov complexity using the MDL principle.

2.2. From quantile scoring to Kolmogorov Complexity

For a distribution F , the Kolmogorov complexity $K(F)$ is the length of the shortest computer program producing F as an output. This concept can be leveraged for causal discovery through the following theorem:

Theorem 2 (Mooij et al. 2010). *Let X and Y be two random variables. If X is a cause of Y , then $K(F_X) + K(F_{Y|X}) \leq K(F_Y) + K(F_{X|Y})$ holds, up to an additive constant.*

Stated differently, the most likely causal direction between X and Y can be recognized by the lowest value of the Kolmogorov complexity. Since the Kolmogorov complexity is not computable, we use the MDL principle, known as the practical version of Kolmogorov complexity, as a proxy. According to the MDL principle, the “best” model is the one providing an optimal compression of the data, i.e., to store information using the shortest code length (CL).

In general, the CL can be decomposed into two parts: the CL of the model under consideration and the leftover information, not explained by the model (see e.g., Hansen and Yu, 2001a). As such, for a given quantile level τ , we can write

$$\begin{aligned} CL_X(\tau) &= CL(\hat{F}_X) + CL(E_Y, \tau), \\ CL_{Y|X}(\tau) &= CL(\hat{F}_{Y|X}) + CL(E_{Y|X}, \tau), \end{aligned}$$

¹We say that $W \sim AL(\tau)$ if the density of W is $f(w; \tau) = \tau(1 - \tau) \exp(-S_\tau(0, w))$.

with \hat{F}_X and $\hat{F}_{Y|X}$ the estimated marginal and conditional distributions,

$$E_X = \{X_i - \hat{F}_X^{-1}(\tau)\}_{i=1}^n,$$

$$E_{Y|X} = \{Y_i - \hat{F}_{Y|X}^{-1}(X_i, \tau)\}_{i=1}^n,$$

and similarly for $CL_Y(\tau)$ and $CL_{X|Y}(\tau)$. Then, according to Theorem 2 and using CL s as proxies for Kolmogorov complexities, if X is a cause of Y , then one expects that

$$CL_{Y|X}(\tau) + CL_X(\tau) \leq CL_{X|Y}(\tau) + CL_Y(\tau).$$

In order to relate asymmetries in CL s to asymmetries in quantile scores (QSs), we make two assumptions:

(A1) F is absolutely continuous, $\{(X_i, Y_i)\}_{i=1}^n$ with $(X_i, Y_i) \sim F$ is an i.i.d. sample, and \hat{F} is an estimator of F based on $\{(X_i, Y_i)\}_{i=1}^n$.

(A2) $\hat{F}_X, \hat{F}_Y, \hat{F}_{X|Y}, \hat{F}_{Y|X}$ derived from \hat{F} are estimators of $F_X, F_Y, F_{X|Y}, F_{Y|X}$. While (A1) is straightforward, (A2) can be understood by noticing that $F_X(x) = F(x, \infty)$, $F_Y(y) = F(\infty, y)$, $F_{X|Y}(x, y) = \partial_y F(x, y) / \partial_y F(x, y)|_{x \rightarrow \infty}$, $F_{Y|X}(x, y) = \partial_x F(x, y) / \partial_x F(x, y)|_{y \rightarrow \infty}$. Then (A2) means that estimators for the marginal and conditional distributions are obtained by replacing F by \hat{F} and using the same relations. We can then state the following theorem:

Theorem 3. *Under assumptions (A1) and (A2), then*

$$CL_{Y|X}(\tau) + CL_X(\tau) \leq CL_{X|Y}(\tau) + CL_Y(\tau)$$

$$\iff$$

$$\hat{S}_{Y|X}(\tau) + \hat{S}_X(\tau) \leq \hat{S}_{X|Y}(\tau) + \hat{S}_Y(\tau),$$

where $\hat{S}_X(\tau) = \sum_{i=1}^n S(\hat{F}_X^{-1}(\tau), X_i)$, $\hat{S}_{Y|X}(\tau) = \sum_{i=1}^n S(\hat{F}_{Y|X}^{-1}(X_i, \tau), Y_i)$ and similarly for Y and $X|Y$.

Stated differently, Theorem 3 implies that there is an equivalence between minimizing code length and quantile score. Hence, because of the MDL principle, the causal direction can be inferred from the lowest quantile score. The proof can be found in the supplementary material. Note that Theorem 3 does not state that CL s and QS s are equivalent, but rather that inequalities in CL s imply inequalities in QS s (and conversely) with respect to a specific statistical model.

Due to stability (or invariance) of the true causal model given different values of the conditioning variable, we expect the outputs of our causal rule to agree over different quantile levels. However, since a single quantile is generally not enough to characterize a distribution, we further consider $\hat{S}_X = \int_{[0,1]} \hat{S}_X(\tau) d\tau$, $\hat{S}_{Y|X} = \int_{[0,1]} \hat{S}_{Y|X}(\tau) d\tau$, and similarly for Y and $X|Y$. By pooling results at different quantile levels, we aim at better describing the marginal and conditional distributions.

Following Budhathoki and Vreeken (2017), we use a normalization based on the sum of the description lengths for the marginal distributions, and define our quantile-based score as

$$S_{X \rightarrow Y} = \frac{\widehat{S}_X + \widehat{S}_{Y|X}}{\widehat{S}_X + \widehat{S}_Y}. \quad (1)$$

We can then equivalently define $S_{Y \rightarrow X}$ by replacing \widehat{S}_X and $\widehat{S}_{Y|X}$ by \widehat{S}_Y and $\widehat{S}_{X|Y}$ in the numerator, and formulate the following rule.

Corollary 1 (Quantile-based causal discovery). *If $S_{X \rightarrow Y} < S_{Y \rightarrow X}$, conclude that X causes Y . If $S_{X \rightarrow Y} > S_{Y \rightarrow X}$, conclude that Y causes X . Otherwise, do not decide.*

Note that proving consistency of this decision rule has to be done relatively to both the class of distributions to which F belongs as well as the estimator \widehat{F} . However, when (A1) and (A2) are satisfied, and \widehat{F} , \widehat{F}_X , \widehat{F}_Y , $\widehat{F}_{X|Y}$, $\widehat{F}_{Y|X}$ are consistent, then proving consistency of the decision rule is straightforward. Regarding identifiability, Theorem 3 uses less than or equal, with equality corresponding to the nonidentifiable cases (such as linear mechanisms with Gaussian noise).

Finally, we use averaging through integration rather than the maximal QS difference over quantile levels because the scale of QS is not uniform over quantile levels (e.g., the closer to 0.5 the higher). Hence, using maximization would essentially mean basing the decision on the median only.

2.3. Intuition

To provide additional intuition for the proposed method, we revisit the reasoning linking Kolmogorov complexity to quantile scoring. As previously discussed, since Kolmogorov complexity is not computable, Theorem 2 cannot be used directly and a proxy must be employed to infer the causal direction. Rissanen (1978) suggests such a proxy by restricting the search to descriptions corresponding to probability distributions. His MDL principle, namely selecting the encoding producing the shortest description of the data, amounts at

- viewing statistical models as mechanisms to generate descriptions of observed data,
- and using code lengths (CLs) as discriminators between competing statistical models.

Furthermore, it coincides with maximum likelihood estimation. Since, by Theorem 2, the causal factorization of the joint distribution has lower complexity, it follows that the true causal model can be inferred as the one having the shortest CL.

In the context of quantile regression, it is common to assume that the errors (the differences between observed values and conditional quantiles) follow an

asymmetric Laplace (AL) distribution (Koenker and Machado, 1999). The reason is that the quantile score is related to the AL likelihood through $\loglik = n \times \log(\tau/(1-\tau)) - n \times QS$. Hence, the AL distribution naturally encodes the errors and $CL \approx -\loglik \approx n \times QS$ where \approx is up to a constant in τ . Intuitively, the likelihood corresponding to (conditional) prediction errors in the causal direction is higher, that is the QS and CL are smaller: the shortest CL corresponds to the largest AL likelihood/smallest QS, which establishes a link between minimizing QS and the MDL principle.

To illustrate this idea, Figure 1 shows a toy example with $Y = 2 \tanh(X) + N(0, 1)$ for the 0.1, 0.5, 0.9 quantile levels. In Figure 2, we show the density of the AL distribution corresponding to the residuals (e.g., $X - F_X^{-1}(\tau)/Y - F_{Y|X}^{-1}(X, \tau)$ for the marginal/conditional distributions in the causal directions). In Figure 1, we observe that QS is indeed smaller for the causal direction. In other words, the correct direction has a higher AL likelihood.

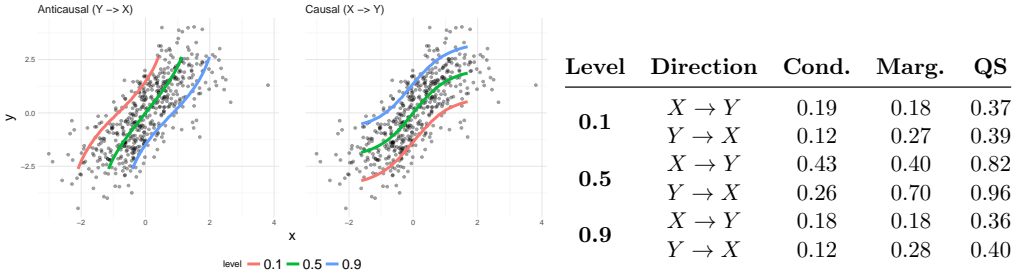


Figure 1: Toy example - asymmetry in (a) fitted models, (b) quantile scores.

2.4. Predicting quantiles with copulas

To leverage Theorem 3 and Corollary 1 for causal discovery, a model of F , the joint distribution of X and Y is required. Furthermore, it has to yield computable expressions for all conditional quantiles. While not the only statistical model satisfying this condition, copulas (i.e., multivariate distributions with uniform margins), represent an appealing alternative.

According to the theorem of Sklar (1959), any F can be represented by its marginal distributions F_X, F_Y and a copula C , which is the joint distribution of $(U, V) = (F_X(X), F_Y(Y))$. In other words, for any F , there exists a C such that $F(x, y) = C(F_X(x), F_Y(y))$ for each $(x, y) \in \mathbb{R}^2$. Moreover, if all the distributions are continuous, then C is unique.

Following Joe (1996), copulas lead to a useful representation of the distributions of $Y|X$ and $X|Y$, namely $F_{Y|X}(x, y) = P(Y \leq y|X = x) = P(V \leq v|U = u) = \partial_u C(u, v)$ where $\partial_u C(u, v) = \partial C(u, v)/\partial u$, $u = F_X(x)$, and $v = F_Y(y)$, and similarly $F_{X|Y}(x, y) = \partial_v C(u, v)$. This means that conditional distributions can

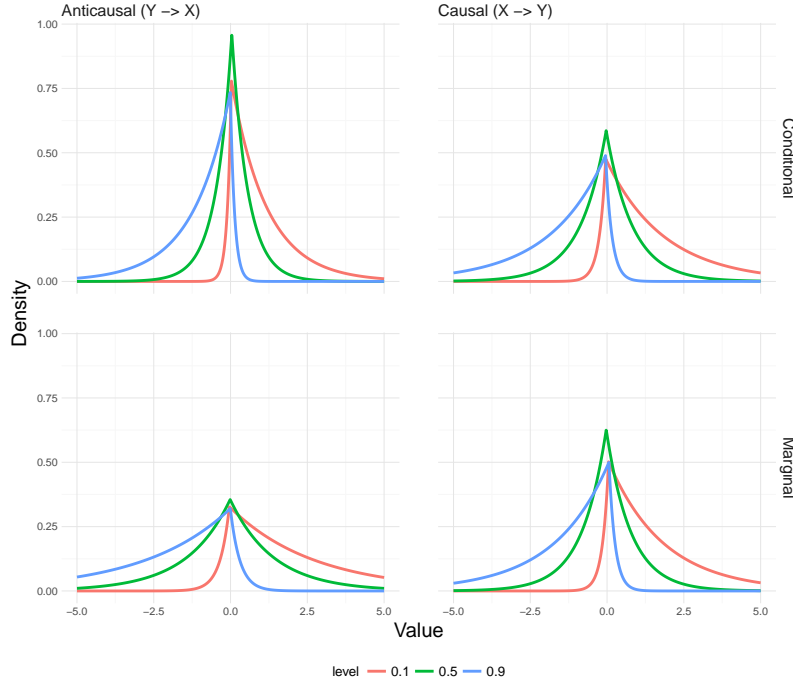


Figure 2: Asymmetric Laplace density corresponding to the residuals from the Example in Figure 1.

be evaluated by taking partial derivatives of the copula function. The τ -quantiles of $Y|X$ can then be written as

$$F_{Y|X}^{-1}(x, \tau) = F_Y^{-1}((\partial_u C)^{-1}(u, \tau)), \quad (2)$$

and similarly for $F_{X|Y}^{-1}(\tau, y)$, with inverse functions of the copula derivatives are with respect to τ . Using (2), one can then compute all τ -quantiles using the marginal distributions and the copula.

3. Estimation and implementation

3.1. Estimation

Assume that we have n i.i.d. random variables $\{(X_1, Y_1), \dots, (X_n, Y_n)\}$. To avoid relying on restrictive assumptions, $S_{X \rightarrow Y}$ and $S_{Y \rightarrow X}$ are estimated completely nonparametrically.

Note that, if all the considered distributions are differentiable, $F(x, y) = C(F_X(x), F_Y(y))$ implies

$$f(x, y) = c\{F_X(x), F_Y(y)\} f_X(x) f_Y(y), \quad (3)$$

where f, c, f_X , and f_Y are the densities corresponding to F, C, F_X , and F_Y re-

spectively. Equation (3) has an important implication for inference: because the right-hand side is a product, the joint log-likelihood can be written as a sum of the log-likelihood of each margin and the log-likelihood of the copula. This fact can be conveniently exploited in a two-step procedure: estimate the margins separately to obtain \hat{F}_X and \hat{F}_Y , and then take the probability integral transform of the data using those margins, that is, define $\hat{U}_i = \hat{F}_X(X_i)$ and $\hat{V}_i = \hat{F}_Y(Y_i)$, to estimate \hat{C} .

For the first step, we simply use the empirical distribution

$$\hat{F}_X(x) = \sum_{i=1}^n \mathbb{I}\{X_i \leq x\} / (n+1)$$

(and similarly for Y), where $n+1$ is used instead of n in the copula context to avoid boundary problems. Discrete datasets are handled by *jittering*, that is breaking ties at random. As for the second step, since typical nonparametric estimators are targeted at densities with unbounded support, they are unsuited to densities restricted to $[0, 1]^2$. To get around this issue, Scaillet et al. (2007) suggests to first transform the data to standard normal margins, and then use any nonparametric estimator suited to unbounded densities. The transformation estimator of the copula density $c(u, v)$ is then defined as

$$\hat{c}(u, v) = \frac{\hat{g}(\Phi^{-1}(u) - \Phi^{-1}(\hat{U}_i), \Phi^{-1}(v) - \Phi^{-1}(\hat{V}_i))}{\phi(\Phi^{-1}(u))\phi(\Phi^{-1}(v))}, \quad (4)$$

where $\hat{U}_i = \hat{F}_X(X_i)$, $\hat{V}_i = \hat{F}_Y(Y_i)$, \hat{g} is a bivariate nonparametric estimator, and ϕ, Φ denote the standard normal density and distribution, respectively.

Denoting $Z_i = (\Phi^{-1}(\hat{U}_i), \Phi^{-1}(\hat{V}_i))$ and $z = (\Phi^{-1}(u), \Phi^{-1}(v))$, the goal is to obtain the density for any $z = (z_1, z_2) \in \mathbb{R}^2$ from the sample $\{Z_i\}_{i=1}^n$ with $Z_i = (Z_{i,1}, Z_{i,2})$. With the bivariate Gaussian kernel

$$W_{B_n}(z_2, z_2) = \exp(-z^\top B_n^{-1} z / 2) / (2\pi \det(B_n)^{1/2})$$

for a positive definite bandwidth matrix B_n , Scaillet et al. (2007) suggests plugging in the kernel estimator $\hat{g}(z_1, z_2) = \sum_{i=1}^n W_{B_n}(z_1 - Z_{i,1}, z_2 - Z_{i,2}) / n$ into (4). The consistency and asymptotic normality of this estimator are derived in Geenens et al. (2017) under assumptions described in the supplementary material, (Section A.2).

3.2. Implementation

The transformation kernel estimator for bivariate copula densities is implemented in C++ as part of **vinecopulib** (Nagler and Vatter, 2017), a header-only C++ library for copula models based on **Eigen** (Guennebaud et al., 2010) and **Boost** (Schäling, 2011). From (4), **vinecopulib** constructs and stores a 30×30 grid

over $[0, 1]^2$ along with the evaluated density at the grid points². Then, a cubic-spline approximation makes it possible to efficiently compute the copula distribution $\hat{C}(u, v)$ and its derivatives, $\partial_u \hat{C}(u, v)$ and $\partial_v \hat{C}(u, v)$, as the integrals of the spline-approximation of the density admits an analytic expression. Finally, **vinecopulib** implements the numerical inversion of $\partial_u \hat{C}(u, v)$ and $\partial_v \hat{C}(u, v)$ to compute $(\partial_u \hat{C})^{-1}(u, v)$ and $(\partial_v \hat{C})^{-1}(u, v)$ by a vectorized version of the bisection method.

The second step of the implementation consists of estimating $S_{Y|X}(\tau)$, $S_{X|Y}(\tau)$, and $S_{X \rightarrow Y}$, namely, plugging in estimates of the marginal and derivatives of the copula in (2) and the scoring function of Example 2. Note that, to compute scores free of scale bias, all variables are transformed to the standard normal scale.

As for estimating the final scores, we use Legendre quadrature to approximate the integral over $[0, 1]$, as it is fast and precise for univariate functions. In other words, denoting by $\{w_j, \tau_j\}_{j=1}^m$ the m pairs of quadrature weights and nodes, we use $\int_0^1 g(\tau) d\tau \approx \sum_{j=1}^m w_j g(\tau_j)$, which when plugged into (1) yields $\hat{S}_X = \sum_{j=1}^m w_j \hat{S}_X(\tau_j)$, $\hat{S}_Y = \sum_{j=1}^m w_j \hat{S}_Y(\tau_j)$, $\hat{S}_{X|Y} = \sum_{j=1}^m w_j \hat{S}_{X|Y}(\tau_j)$, and $\hat{S}_{Y|X} = \sum_{j=1}^m w_j \hat{S}_{Y|X}(\tau_j)$. Note that summing over an equally spaced grid with uniform weights or using quadrature nodes and weights yields two valid approximations of an integral, and using one or the other should not matter. However, the quadrature gives more importance to the center of the distribution (i.e., quantiles closer to 0.5 have a higher weight).

QCCD is implemented using the R interface (R Core Team, 2017) interface to **vinecopulib** called **rvinecopulib** (Nagler and Vatter, 2018) and Gauss-Legendre quadrature from the package **statmod** (Smyth, 2005). The procedure is summarized as an algorithm in the supplementary material, (Section B.1).

Computational complexity QCCD scales linearly with the size of input data as well as the number of quantiles used in the quadrature, that is the overall complexity is $\mathcal{O}(nm)$. As such, QCCD compares favorably to nonparametric methods relying on computationally intensive procedures, for an instance based on kernels (Chen et al., 2014, Hernández-Lobato et al., 2016) or Gaussian processes (Hoyer et al., 2009, Mooij et al., 2010, Sgouritsa et al., 2015). The parameter m can be used to control for the trade-off between the computational complexity and the precision of the estimation. We recommend the value $m = 3$ which, makes it possible to capture variability in both location and scale. Setting $m = 1$ is essentially equivalent to using only the conditional median for causal discovery, a setting that suitable for distributions with constant variance. An empirical analysis of the choice of m is provided in the following section. In what follows,

² After extensive simulations comparing copula densities to their kernel approximations, the authors of **vinecopulib** noticed that the precision gains achieved by increasing beyond 30×30 were marginal. Using a grid is not actually required to implement the kernel-based estimator, but evaluating kernels for each call to the copula's density is computationally expensive and storing the values is a time-memory trade-off.

we report results for QCCD with $m = 3$ if not stated otherwise.

4. Experiments

Benchmarks For simulated data, we first rely on the following scenarios (Mooij et al., 2016): *SIM* (without confounder), *SIM-ln* (with low noise), *SIM-G* (with distributions close to Gaussian), and *SIM-c* (with latent confounder). There are 100 pairs of size $n = 1000$ in each of these datasets.

The second experiment, inspired by Peters et al. (2014), studies nonlinear additive noise (*AN*) models of the form $Y = f(X) + E_Y$ for some deterministic function f with $E_Y \sim \mathcal{N}(0, \sigma)$, $X \sim \mathcal{N}(0, \sqrt{2})$, and $\sigma \sim \mathcal{U}[1/5, \sqrt{2/5}]$. In *AN*, f is an arbitrary nonlinear function simulated using Gaussian processes (GP, Rasmussen and Williams, 2006) with a Gaussian kernel of bandwidth one. Since the functions in *AN* are often non-injective, we include *AN-s* to explore the behavior of QCCD in injective cases. In this setup, f are sigmoids as in (Bühlmann et al., 2014). The third experiment considers location-scale (*LS*) data generating processes with both the mean and variance of the effect being functions of the cause, that is $Y = f(X) + g(X)E_Y$, and E_Y and X are similar as for the additive noise models. *LS* and *LS-s* then correspond to the Gaussian processes and sigmoids described for *AN* and *AN-s*. Finally, the fourth experiment considers multiplicative models (*MN*) as $Y = f(X)E_Y$, with $f(X)$ sampled as sigmoid functions and $E_Y \sim \mathcal{U}(0, 1)$. In each of the second, third, and fourth experiments, we simulate 100 pairs of size $n = 1000$. All pairs have equal weights with variable ordering according to a coin flip, therefore resulting in balanced datasets. Example datasets for each of the simulated experiments are shown in the supplementary material, (Section E).

For real data, we use the Tübingen CE benchmark (version Dec 2017), consisting of 108 pairs from 37 different domains, from which we consider only the 99 pairs that have univariate continuous or discrete cause and effect variables. When evaluating the performance on this dataset we included the pairs' corresponding weights which accounts for potential bias in cases where pairs were selected from same multivariable dataset.

Baselines On simulated data, we compare QCCD to state-of-the-art approaches, namely RESIT (Peters et al., 2014), biCAM (Bühlmann et al., 2014), LinGaM (Shimizu et al., 2006), and GR-AN (Hernández-Lobato et al., 2016), which are ANM-based, and IGCI (Janzing and Schölkopf, 2010), EMD (Chen et al., 2014), and Slope (Marx and Vreeken, 2017), which are based on the independence postulate.

We also consider other methods such as PNL-MLP (Zhang and Hyvärinen, 2009), GPI (Mooij et al., 2010), ANM (Hoyer et al., 2009), and CURE (Sgouritsa et al., 2015). For the real data benchmark, GR-AN was evaluated over 15 subsamples limited to 500 observations, and the results are then averaged. Implementation details and hyper parameters for all baselines are described in the

supplementary material, (Section B.2).

Our code and datasets are available on the following link.

Evaluation metrics As Mooij et al. (2016), we use the *accuracy* for *forced decisions* and the *area under the receiver operating curve* (ROC) for *ranked decisions*. As a confidence heuristic for the ranked decisions for QCCD, we use same score as (24) in (Mooij et al., 2016), that is $\hat{C} = -S_{X \rightarrow Y} + S_{Y \rightarrow X}$.

Selection of m In the experiments on simulated datasets, we also investigate the significance of the parameter m with regards to different sample sizes. Looking at the figures in Figure 3, we can clearly see in which cases multiple quantile levels can indeed increase the accuracy, namely for sigmoid (i.e., harder to detect) causal mechanisms. For confounded data, increasing m seems to help too, albeit faintlier. Additionally, we can notice that higher values of m have more pronounced effect as the sample size increases. This was used to improve our results on real data, namely by setting the parameter m to 1 when $n < 200$ and $m = 3$ for the rest.

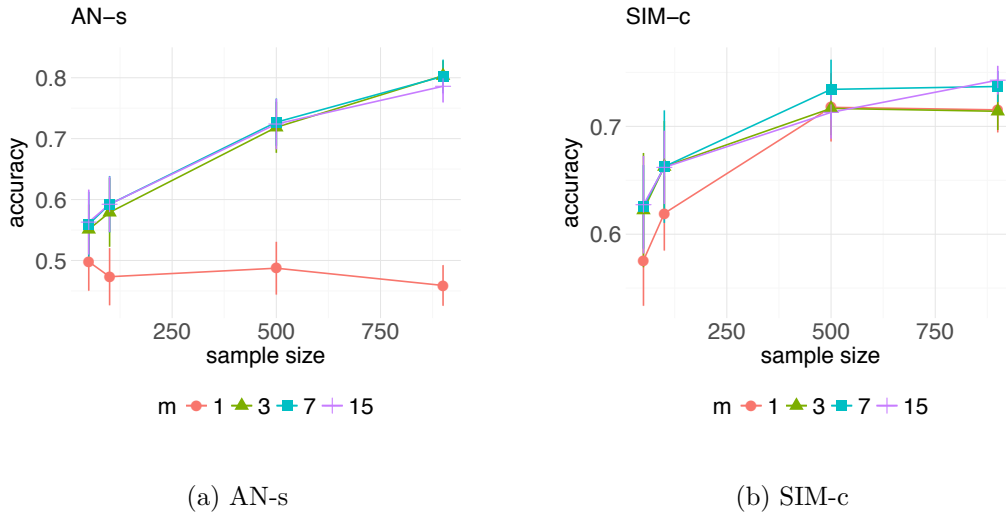


Figure 3: Accuracy in function of m and sample size.

Results and discussion In Figure 4, we compare the causal discovery algorithms across simulated datasets with regards to accuracy, and no single baseline is an overall best performer. Tabulated numbers can be found in the supplementary material.

Starting with the SIM benchmarks, we notice that GPI achieves highest accuracy in all four scenarios, followed with similar results by RESIT/ANM ³. On

³Because RESIT is an R version based on the MATLAB ANM, we overlay their results on a single chart.

this benchmark, QCCD behaves similarly to the rest of the baselines, while being more robust in the confounded scenario where others achieve results on the scale of random guess. Interestingly, higher values of the parameter m improve the results in such pairs.

The results are significantly different for the AN, LS and MN scenarios. biCAM, ANM and RESIT easily handle the AN pairs since their underlying assumptions are met, while we can notice some discrepancy in the LS and MN scenarios where there is an interaction between the noise and the cause. Similarly, LINGAM does not perform well on any of the datasets, which are all highly nonlinear, hence violating its assumptions. IGCI can handle any scenario with the gaussian reference measure, while this is not the case with the uniform measure⁴. In the LS generative models where not only the mean, but the variance of the effect changes with the cause only IGCI-g was on-par with QCCD, but QCCD is still better than IGCI-g on the SIM benchmark and real data pairs. On the other hand, more flexible methods such as PNL and EMD had difficulties in the non-injective cases. QCCD has satisfactory ($> 75\%$ accuracy) for all different data generative mechanisms (AN, LS and MN). Looking at the ROC curves in Figure 5a, we notice that QCCD performs better than a random classifier on all benchmarks.

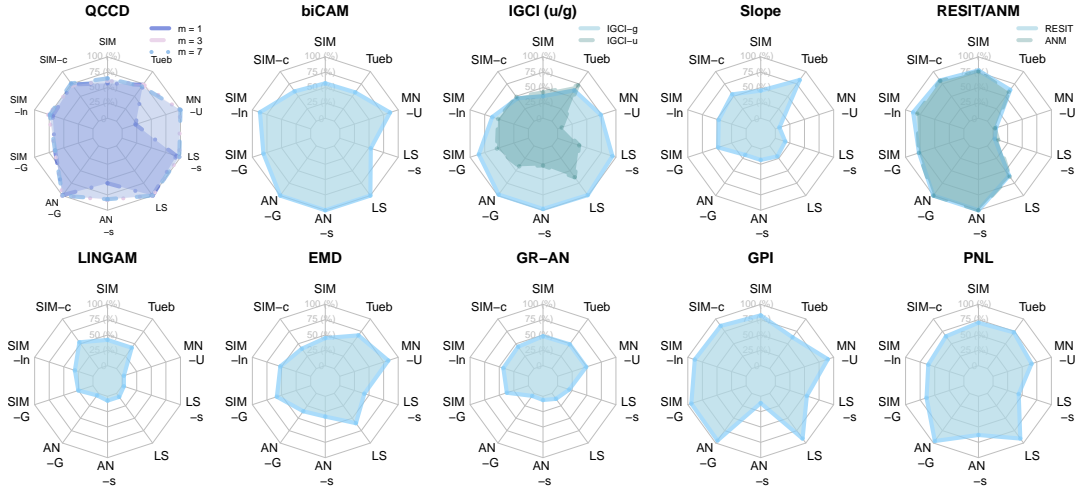


Figure 4: Accuracy of QCCD and competitors.

With real data pairs, Table 1 shows that that QCCD⁵ is highly competitive in terms of weighted accuracy, with only Slope achieving better overall results. Additionally, we include ROC curves and accuracy decision-rate plot in Figure 5. Note that QCCD provides statistically significant results (i.e., compared to a coin flip) and is second out of the 6 best performing algorithms with respect to weighted accuracy. In the supplementary material, we further provide accuracy

⁴Note that selecting the reference measure is the most sensitive part of the method and is as difficult as selecting the right kernel/bandwidth for a specific task (Janzing et al., 2012, Mooij et al., 2016).

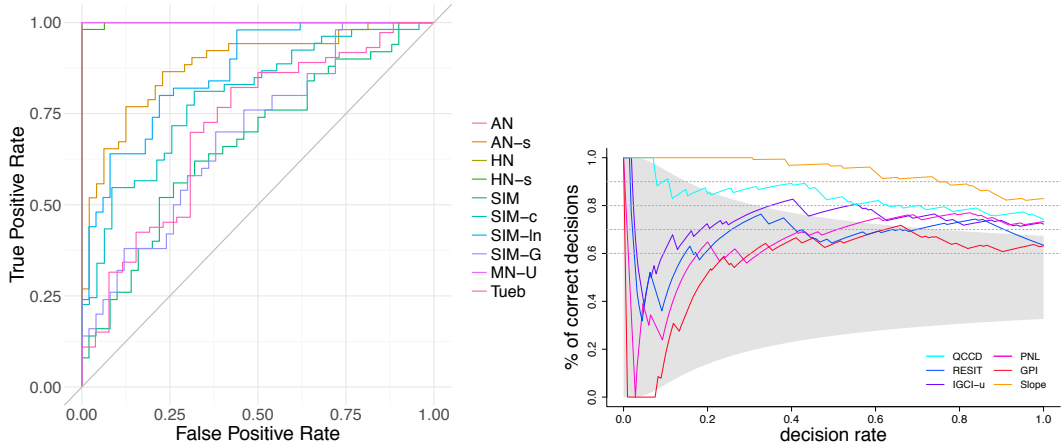
⁵Results are averaged over 30 repetitions to account for the effect of the jittering in the discrete pairs.

decision rate plot and ROC curves with all baselines. Moreover, the efficiency of our method is highlighted in the last row of Table 1, where QCCD is able to go over the whole dataset in ~ 7 minutes. As for other nonparametric methods, only IGCI is faster, Slope is twice as slow, RESIT 55 times, PNL 71 times, and the others required days to go through the whole dataset or had to be averaged on subsamples due to slow execution (GRAN).

Overall, we can conclude that compared to baselines QCCD performs well in both real and simulated scenarios therefore being more robust to different generative models while also having computational advantages compared to the other baselines.

Table 1: Results for the Tübingen benchmark (rounded standard deviations in parentheses).

	QCCD	IGCI-u/g	biCAM	Slope	LINGAM	RESIT
Acc	0.68(1.6)	0.67/0.61	0.57	0.75	0.3	0.53
Weighted Acc.	0.75(0.02)	0.72/0.62	0.58	0.83	0.36	0.63
Area Under ROC	0.71(0.01)	0.67	0.61	0.84	0.3	0.56
CPU	7 min.	2 sec.	10 sec.	25 min.	3.5 sec.	12 h
	EMD	GRAN	GPI	PNL-MLP	ANM	CURE
Acc	0.55	0.4 (2.2)	0.6	0.75	0.6	0.6
Weighted Acc.	0.6	0.5 (0.02)	0.63	0.73	0.6	0.54
Area Under ROC	0.53	0.47 (0)	0.61	0.7	0.45	0.61
CPU	4.6 days	NA	30 days	8.3 h	3.2 days	NA



(a) ROC curves for QCCD on all benchmarks. (b) Accuracy decision-rates for the top 6 baselines on the Tübingen benchmark.

Figure 5: Ranked decision evaluations.

5. Conclusion

In this work, we develop a causal discovery method based on conditional quantiles. We give a rigorous basis to the approach by showing its link to Kolmogorov

complexity and therefore to the independence postulate. We propose QCCD, an effective implementation of our method based on nonparametric copulas. Studying QCCD extensively both with simulated and real datasets, we show that it compares favorably to state-of-the-art methods showing consistent results under different functional models and statistically significant results on real data. There are currently two directions that we are exploring to extend this work. First, our theory allows for a modular approach to pairwise causal discovery: using different combinations of quantile regression approaches and consistent quantile scoring functions could improve the results in cases where QCCD has limited power. Second, the computational efficiency of QCCD is promising in the context of extensions to higher dimensional datasets. As such, ongoing research leverages existing graph discovery algorithms for hybrid learning, as suggested in the supplementary material. Furthermore, using QCCD and pair-copula constructions as building blocks for a novel approach to learn functional causal models is a promising area for further work.

References

- (2015). Structural Intervention Distance for Evaluating Causal Graphs. *Neural Computation*, 27(3):771–799.
- Aue, A., Cheung, R. C. Y., Lee, T. C. M., and Zhong, M. (2014). Segmented model selection in quantile regression using the minimum description length principle. *Journal of the American Statistical Association*, 109(109):507–1241.
- Bauer, A. and Czado, C. (2016). Pair-copula Bayesian networks. *Journal of Computational and Graphical Statistics*, 25(4):1248–1271.
- Budhathoki, K. and Vreeken, J. (2017). Causal inference by compression. In *ICDM*, pages 41–50.
- Bühlmann, P., Peters, J., and Ernest, J. (2014). CAM: Causal additive models, high-dimensional order search and penalized regression. *Annals of Statistics*, 42(6):2526–2556.
- Chang, Y., Li, Y., Ding, A., and Dy, J. (2016). A robust-equitable copula dependence measure for feature selection. *AISTATS*, 41:84–92.
- Chen, Z., Zhang, K., Chan, L., and Schölkopf, B. (2014). Causal discovery via reproducing kernel hilbert space embeddings. *Neural Computation*, 26(7):1484–1517.
- Cui, R., Groot, P., and Heskes, T. (2016). Copula PC algorithm for causal discovery from mixed data. In *Lecture Notes in Computer Science (including subseries Lecture Notes in Artificial Intelligence and Lecture Notes in Bioinformatics)*, volume 9852 LNAI, pages 337–392. Springer, Cham.
- Elidan, G. (2013). Copulas in machine learning. In *Copulae in mathematical and quantitative finance*, pages 39–60. Springer.
- Embrechts, P., Mcneil, E., and Straumann, D. (1999). Correlation: Pitfalls and alternatives. *Risk Magazine*.
- Fisher, R. A. (1936). Statistical methods for research workers. *Especially Section*, 21.
- Geenens, G., Charpentier, A., and Paindaveine, D. (2017). Probit transformation for nonparametric kernel estimation of the copula density. *Bernoulli*, 23(3):1848–1873.
- Geraci, M. and Bottai, M. (2006). Quantile regression for longitudinal data using the asymmetric laplace distribution. *Biostatistics*, 8(1):140–154.
- Gneiting, T. (2011). Making and evaluating point forecasts. *Journal of the American Statistical Association*, 106(494):746–762.

- Goudet, O., Kalainathan, D., Caillou, P., Lopez-Paz, D., Guyon, I., Sebag, M., Tritas, A., and Tubaro, P. (2017). Learning functional causal models with generative neural networks. *preprint*. arXiv: 1709.05321.
- Guennebaud, G., Jacob, B., and Others (2010). Eigen v3.
- Hansen, M. H. and Yu, B. (2001a). Model selection and the principle of minimum description length. *Journal of the American Statistical Association*, 96(454):746–774.
- Hansen, M. H. and Yu, B. (2001b). Model selection and the principle of minimum description length. *Journal of the American Statistical Association*, 96(454):746–774.
- Harris, N. and Drton, M. (2013). PC Algorithm for nonparanormal graphical models. *Journal of Machine Learning Research*, 14:3365–3383.
- Heinze-Deml, C., Peters, J., and Meinshausen, N. (2017). Invariant causal prediction for nonlinear models. *preprint*. arXiv: 1706.08576.
- Hernández-Lobato, D., Morales Mombiela, P., Lopez-Paz, D., and Suárez, A. (2016). Non-linear causal inference using Gaussianity measures. *Journal of Machine Learning Research*, 17(1):939–977.
- Hoyer, P. O., Janzing, D., Mooij, J., Peters, J., and Schölkopf, B. (2009). Nonlinear causal discovery with additive noise models. In *NIPS 22*, pages 689–696.
- Janzing, D., Mooij, J., Zhang, K., Lemeire, J., Zscheischler, J., Daniušis, P., Steudel, B., and Schölkopf, B. (2012). Information-geometric approach to inferring causal directions. *Artificial Intelligence*, 182:1–31.
- Janzing, D. and Schölkopf, B. (2010). Causal Inference using the algorithmic markov condition. *IEEE Transactions on Information Theory*, 56(10):5168–5194.
- Joe, H. (1996). Families of m-variate distributions with given margins and $m(m-1)/2$ bivariate dependence parameters. In *Distributions with fixed marginals and related topics*, pages 120–141. Institute of Mathematical Statistics.
- Koenker, R. and Machado, J. A. (1999). Goodness of fit and related inference processes for quantile regression. *Journal of the american statistical association*, 94(448):1296–1310.
- Kolmogorov, A. N. (1963). On tables of random numbers. *Sankhyā: The Indian Journal of Statistics, Series A*, pages 369–376.
- Liu, F. and Chan, L.-W. (2017). Causal inference on multidimensional data using free probability theory. *IEEE Transactions on Neural Networks and Learning Systems*.

- Liu, H., Lafferty, J., and Wasserman, L. (2009). The Nonparanormal: semiparametric estimation of high dimensional undirected graphs. *Journal of Machine Learning Research*, 10:2295–2328.
- Lopez-Paz, D. (2016). *From Dependence to Causation*. PhD thesis, University of Cambridge.
- Lopez-Paz, D., Hernandez-Lobato, J. M., and Schölkopf, B. (2013). Semi-supervised domain adaptation with copulas. *NIPS 26*, pages 674–682.
- Lopez-Paz, D., Muandet, K., Schölkopf, B., and Tolstikhin, I. (2015). Towards a learning theory of cause-effect inference. In *ICML 32*, pages 1452–1461.
- Maathuis, M. H. and Nandy, P. (2016). A review of some recent advances in causal inference. In *Handbook of Big Data*. CRC Press.
- Marx, A. and Vreeken, J. (2017). Telling cause from effect using MDL-based local and global regression. In *ICDM*.
- Mooij, J. M., Peters, J., Janzing, D., Zscheischler, J., and Schölkopf, B. (2016). Distinguishing cause from effect using observational data: methods and benchmarks. *Journal of Machine Learning Research*, 17:1–102.
- Mooij, J. M., Stegle, O., Janzing, D., Zhang, K., and Schölkopf, B. (2010). Probabilistic latent variable models for distinguishing between cause and effect. In *NIPS 23*, pages 1687–1695.
- Müller, D. and Czado, C. (2017). Selection of sparse vine copulas in high dimensions with the lasso.
- Nagler, T. and Vatter, T. (2017). vinecopulib: High Performance Algorithms for Vine Copula Modeling in C++. <http://vinecopulib.org>.
- Nagler, T. and Vatter, T. (2018). rvinecopulib: high performance algorithms for vine copula modeling.
- Pearl, J. (2009). *Causality*. Cambridge University Press.
- Pearl, J., Glymour, M., and Jewell, N. P. (2016). *Causal Inference in Statistics: A Primer*. John Wiley & Sons.
- Peters, J. and Ernest, J. (2015). *CAM: Causal Additive Model (CAM)*.
- Peters, J., Janzing, D., and Schölkopf, B. (2017). *Elements of Causal Inference: Foundations and Learning Algorithms*. MIT Press (available on-line).
- Peters, J., Mooij, J. M., Janzing, D., and Schölkopf, B. (2011). Identifiability of causal graphs using functional models. In *UAI 27*, pages 589–598.

- Peters, J., Mooij, J. M., Janzing, D., and Schölkopf, B. (2014). Causal discovery with continuous additive noise models. *Journal of Machine Learning Research*, 15(1):2009–2053.
- Pircalabelu, E., Claeskens, G., and Gijbels, I. (2017). Copula directed acyclic graphs. *Statistics and Computing*, 27(1):55–78.
- R Core Team (2017). R: A language and environment for statistical computing.
- Rasmussen, C. E. and Williams, C. K. I. (2006). *Gaussian Processes for Machine Learning*, volume 1. MIT Press Cambridge.
- Rissanen, J. (1978). Modeling by shortest data description. *Automatica*, 14(5):465–471.
- Sachs, K., Perez, O., Pe’er, D., Lauffenburger, D. A., and Nolan, G. P. (2005). Causal Protein-Signaling Networks Derived from Multiparameter Single-Cell Data. *Science*, 308(5721):523–529.
- Scaillet, O., Charpentier, A., and Fermanian, J.-D. (2007). The estimation of copulas: Theory and practice. Technical report, Ensae-Crest and Katholieke Universiteit Leuven, NP-Paribas and Crest; HEC Genve and Swiss Finance Institute.
- Schäling, B. (2011). *The Boost C++ Libraries*.
- Schölkopf, B., Janzing, D., Peters, J., Sgouritsa, E., Zhang, K., and Mooij, J. (2012). On causal and anticausal learning. In *ICML 29*, pages 1255–1262.
- Sgouritsa, E., Janzing, D., Hennig, P., and Schölkopf, B. (2015). Inference of cause and effect with unsupervised inverse regression. In *AISTATS 38*, pages 847–855.
- Shimizu, S., Hoyer, P., Hyvärinen, Aapo, and Antti, K. (2006). A linear non-gaussian acyclic model for causal discovery. *Journal of Machine Learning Research*, 7:2003–2030.
- Sklar, A. (1959). Fonctions de répartition à n dimensions et leurs marges. *Publications de L’Institut de Statistique de L’Université de Paris*, 8:229–231.
- Smyth, G. K. (2005). Numerical integration. *Encyclopedia of Biostatistics*, pages 3088–3095.
- Spirtes, P. and Zhang, K. (2016). Causal discovery and inference: Concepts and recent methodological advances. *Applied Informatics*, pages 165–191.
- Tran, D., Blei, D. M., and Airolidi, E. M. (2015). Copula variational inference. In *NIPS 28*, pages 3564–3572.

- Tsamardinos, I., Brown, L. E., and Aliferis, C. F. (2006). The max-min hill-climbing Bayesian network structure learning algorithm. *Machine Learning*, 65(1):31–78.
- Turing, A. M. (1937). On computable numbers, with an application to the Entscheidungsproblem. *Proceedings of the London Mathematical Society*, 2(1):230–265.
- Turing, A. M. (1938). On computable numbers, with an application to the Entscheidungsproblem. A correction. *Proceedings of the London Mathematical Society*, 2(1):544–546.
- Yu, K., Lu, Z., and Stander, J. (2003). Quantile regression: applications and current research areas. *Journal of the Royal Statistical Society: Series D (The Statistician)*, 52(3):331–350.
- Zhang, K. and Hyvärinen, A. (2009). On the identifiability of the post-nonlinear causal model. In *UAI 25*, pages 647–655.

A. Theory

A.1. Proof of Theorem 3

The code length CL can be decomposed into two parts: the CL of the model under consideration and the leftover information, not explained by the model (see e.g., Hansen and Yu, 2001b). As such, for a given quantile level τ , we can write:

$$CL_X(\tau) = CL(\hat{F}_X) + CL(E_Y, \tau), \quad CL_Y(\tau) = CL(\hat{F}_Y) + CL(E_X, \tau), \quad (5)$$

$$CL_{X|Y}(\tau) = CL(\hat{F}_{X|Y}) + CL(E_{X|Y}, \tau), \quad CL_{Y|X}(\tau) = CL(\hat{F}_{Y|X}) + CL(E_{Y|X}, \tau),$$

where

$$\begin{aligned} E_X &= \{X_i - \hat{F}_X^{-1}(\tau)\}_{i=1}^n, & E_Y &= \{Y_i - \hat{F}_Y^{-1}(\tau)\}_{i=1}^n, \\ E_{X|Y} &= \{X_i - \hat{F}_{X|Y}^{-1}(\tau, Y_i)\}_{i=1}^n, & E_{Y|X} &= \{Y_i - \hat{F}_{Y|X}^{-1}(X_i, \tau)\}_{i=1}^n. \end{aligned}$$

Thanks to assumption (A2), the conditional and marginal distributions can be derived from the same joint estimator. In other words, since

$$\begin{aligned} \hat{F}_X(x) &= \hat{F}(x, \infty), & \hat{F}_{Y|X}(x, y) &= \partial_x \hat{F}(x, y) / (\partial_x \hat{F}(x, y)|_{y \rightarrow \infty}) \\ \hat{F}_Y(y) &= \hat{F}(\infty, y), & \hat{F}_{X|Y}(x, y) &= \partial_y \hat{F}(x, y) / (\partial_y \hat{F}(x, y)|_{x \rightarrow \infty}), \end{aligned}$$

$\hat{F}_X, \hat{F}_Y, \hat{F}_{X|Y}, \hat{F}_{Y|X}$ are encoded by \hat{F} and thus have the same CL, that is,

$$CL(\hat{F}_X) = CL(\hat{F}_Y) = CL(\hat{F}_{Y|X}) = CL(\hat{F}_{X|Y}) = CL(\hat{F}).$$

Hence, we have that

$$\begin{aligned} CL_{Y|X}(\tau) + CL_X(\tau) &\leq CL_{X|Y}(\tau) + CL_Y(\tau) \\ &\iff \\ CL(E_{Y|X}, \tau) + CL(E_X, \tau) &\leq CL(E_{X|Y}, \tau) + CL(E_Y, \tau). \end{aligned} \quad (6)$$

Furthermore, since quantile scores are related to likelihood estimation (Aue et al., 2014, Geraci and Bottai, 2006, Yu et al., 2003), and because the code length unexplained by a model can be written as its log-likelihood (Hansen and Yu, 2001b), we have that

$$\begin{aligned} CL(E_Y, \tau) &= \hat{S}_X(\tau), & CL(E_X, \tau) &= \hat{S}_Y(\tau), \\ CL(E_{X|Y}, \tau) &= \hat{S}_{X|Y}(\tau), & CL(E_{Y|X}, \tau) &= \hat{S}_{Y|X}(\tau) \end{aligned}$$

Combining this with (A.1) proves the theorem. \square

A.2. Assumptions for the consistency and asymptotic normality of the estimator

- (B1) $\partial_u C(u, v)$ and $\partial_{uu} C(u, v)$ exist and are continuous on $(u, v) \in (0, 1) \times [0, 1]$, and there exists a constant K_1 such that $|\partial_{uu} C(u, v)| \leq K_1/u(1-u)$ for $(u, v) \in (0, 1) \times [0, 1]$.
- (B2) $\partial_v C(u, v)$ and $\partial_{vv} C(u, v)$ exist and are continuous on $(u, v) \in [0, 1] \times (0, 1)$, and there exists a constant K_2 such that $|\partial_{vv} C(u, v)| \leq K_2/v(1-v)$ for $(u, v) \in [0, 1] \times (0, 1)$.
- (B3) The density $c(u, v) = \partial_{uv} C(u, v)$ admits continuous second-order partial derivatives in $(0, 1)^2$ and there exists a constant K_0 such that, for $(u, v) \in (0, 1)^2$, $c(u, v) \leq K_0 \min \left(\frac{1}{u(1-u)}, \frac{1}{v(1-v)} \right)$.

B. Implementation details

B.1. QCCD algorithm

We summarize the QCCD procedure as Algorithm 1 below.

Algorithm 1 QCCD algorithm

Input: i.i.d. observations $\{X_i, Y_i\}_{i=1}^n$
of the r.v. X and Y .

1. Define pseudo-observations by

$$\hat{U}_i = \sum_{j=1}^n \mathbb{I}\{X_j \leq X_i\} / (n+1), \quad \hat{V}_i = \sum_{j=1}^n \mathbb{I}\{Y_j \leq Y_i\} / (n+1).$$

2. Estimate the copula nonparametrically to get

$$h_u(u, v) = (\partial_u \hat{C})^{-1}(u, v), \quad h_v(u, v) = (\partial_v \hat{C})^{-1}(u, v).$$

3. Compute the quadrature weights and nodes $\{w_j, \tau_j\}_{j=1}^m$.

4. Initialize scores $\hat{S}_X \rightarrow 0$, $\hat{S}_Y \rightarrow 0$
 $\hat{S}_{X|Y} \rightarrow 0$, $\hat{S}_{Y|X} \rightarrow 0$.

5. Rescale the variables by defining $X_i = \Phi(U_i)$ and $Y_i = \Phi(V_i)$ for $i = 1, \dots, n$ and Φ the standard normal cumulative distribution.

for $j = 1$ **to** m **do**

$$\begin{aligned} \hat{S}_X &\rightarrow \hat{S}_X + w_j \sum_{i=1}^n S(\hat{F}_X^{-1}(\tau), X_i) / n, & \hat{S}_Y &\rightarrow \hat{S}_Y + w_j \sum_{i=1}^n S(\hat{F}_Y^{-1}(\tau), Y_i) / n \\ \hat{S}_{X|Y} &\rightarrow \hat{S}_{X|Y} + w_j \sum_{i=1}^n S(\hat{F}_X^{-1}(h_u(\tau, \hat{V}_i)), X_i) / n, & \hat{S}_{Y|X} &\rightarrow \hat{S}_{Y|X} + w_j \sum_{i=1}^n S(\hat{F}_Y^{-1}(h_v(\hat{U}_i, \tau)), Y_i) / n. \end{aligned}$$

end for

5. Define $S_{X \rightarrow Y} = (\hat{S}_X + \hat{S}_{Y|X}) / (\hat{S}_X + \hat{S}_Y)$ and $S_{Y \rightarrow X} = (\hat{S}_Y + \hat{S}_{X|Y}) / (\hat{S}_X + \hat{S}_Y)$.

if $S_{Y \rightarrow X} > S_{X \rightarrow Y}$ **then**

Define causal discovery $d = X \rightarrow Y$.

else if $S_{Y \rightarrow X} < S_{X \rightarrow Y}$ **then**

Define causal discovery $d = Y \rightarrow X$.

else

Define causal discovery $d =$
undecided.

end if

Output: (d, s)

B.2. Baselines - Implementations and hyper parameters

For IGCI, we use the original implementation of Janzing et al. (2012) with slope-based estimation with both gaussian and uniform reference measure. For LINGAM, we use the implementation of Peters et al. (2014), which also provides RESIT with GP regression and the HSIC independence test with a threshold value $\alpha = 0.05$. For CAM, we use the R package (Peters and Ernest, 2015) with the default parameters. For GR-AN and EMD, we use the code of Hernández-Lobato et al. (2016). The parameters for EMD on simulated data are as in the

original paper, $\lambda = 1e^{-3}$ and $\sigma = \frac{1}{5}S_m$ (S_m being the median of distances across all input patterns). For the real data, the parameters are tuned and selected from the overall best results. GR-AN has a built-in function that takes care parameter tuning. For Slope, we use the implementation of Marx and Vreeken (2017), with local regression included in the fitting process. For PNL, GPI-MML, and ANM, we use the MATLAB implementation from the *Cause Effect Pairs Challenge FirfiD*, with the same setup as RESIT for ANM.

Our code and datasets used for the paper are included in the submitted supplementary package.

Because there is no publicly available implementation of CURE, we use the results from files obtained by Marx and Vreeken (2017). All experiments are carried out using R version 3.4.1 on a MacBook Pro (mid-2015) with 16GB memory, a 2.2 GHz Intel Core i7 processor and 250GB SSD.

C. Additional results from experiments

Table 2: Accuracy on simulated and real data.

	SIM	SIM-c	SIM-ln	SIM-G	AN	AN-s	LS	LS-s	MN-U	Tüb	Tüb weigh.
QCCD $m = 1$	0.57	0.69	0.69	0.59	0.99	0.47	1	0.93	0.23	0.64	0.74
QCCD $m = 3$	0.61	0.72	0.76	0.65	1	0.81	1	0.98	0.99	0.69	0.77
QCCD $m = 7$	0.65	0.76	0.74	0.66	1	0.82	1	0.98	0.99	0.67	0.75
IGCI - u	0.42	0.49	0.52	0.54	0.41	0.27	0.63	0.37	0.07	0.67	0.72
IGCI - g	0.36	0.46	0.62	0.85	0.98	0.98	0.99	0.94	0.74	0.61	0.64
biCAM	0.57	0.6	0.87	0.81	1	1	1	0.53	0.86	0.57	0.58
Slope	0.45	0.54	0.47	0.48	0.18	0.18	0.21	0.17	0.07	0.75	0.83
RESIT	0.78	0.82	0.87	0.77	1	1	0.6	0.03	0.05	0.53	0.63
ANM	0.76	0.81	0.80	0.77	1	1	0.62	0.09	0.03	0.59	0.59
LINGAM	0.42	0.53	0.31	0.25	0	0.04	0.07	0.03	0	0.27	0.42
EMD	0.45	0.4	0.52	0.58	0.36	0.33	0.6	0.42	0.83	0.6	0.68
GRAN	0.48	0.44	0.43	0.37	0.05	in pr	0.11	0.20	0.5	0.4	0.5
GPI	0.82	0.86	0.88	0.94	0.95	0.11	0.91	0.54	0.90	0.6	0.63
PNL	0.70	0.65	0.61	0.64	0.96	0.63	0.91	0.44	0.66	0.75	0.73

Table 3: Area under the ROC and PR curves for QCCD.

	SIM	SIM-c	SIM-ln	SIM-G	AN	AN-s	LS	LS-s	MN-U
ROC-AUC	0.67	0.79	0.87	0.69	1	0.9	1	1	1
PR-AUC	0.67	0.82	0.86	0.7	1	0.89	1	1	1

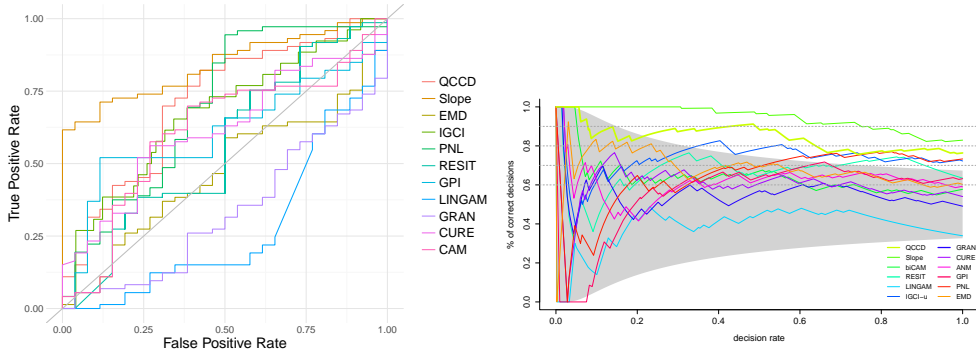


Figure 6: ROC curves and weighted accuracy-decision rate curves for all baselines on the Tübingen dataset.

Note that due to RESIT being undecided in few of the real data pairs, we observe the random classifier behavior at the beginning of its ROC curve in the above plot.

D. Extensions of the pairwise method

Recent work by Goudet et al. (2017) suggests that pairwise and CPDAG (the skeleton and the v -structures of a graphical model) learning procedures can suitably complement each other. In this section, we follow a similar approach to suggest an extension of QCCD to multivariate datasets: start from the CPDAG resulting from another method, and then use QCCD to orient the edges. We rank edges and include them in the graph sequentially, starting from the edge with the highest confidence, while checking the acyclicity of the resulting graph after each addition. Note that this approach also requires a final verification to test edge orientation and v -structures consistency (Goudet et al., 2017).

We explore this idea by using CAM to learn a CPDAG and then QCCD to orient its edges. The rationale is that, while Bühlmann et al. (2014) proves the consistency of CAM to learn the structure when assumptions are not met, QCCD is better in pairwise discoveries (see Section 3).

We now turn to the well know protein causal dataset by Sachs et al. (2005), for which a ground truth DAG of the causal structure is provided. We used the *cd3cd28* dataset with 853 observations of 11 proteins. Once a CPDAG is learned by CAM, we orient the edges using QCCD. For evaluation we use the structural hamming distance (SHD) as proposed in (Tsamardinos et al., 2006) (adding, removing or reversing an edge) necessary to transform one graph to the another and the structural intervention distance (SID), as in (Pet, 2015), which is considered to be appropriate for quantifying the correct order among variables, by estimating the causal effects they entail. CAM by itself outputs a DAG with $SID_{CAM} = 53$, and $SHD_{CAM} = 17$, while with QCCD we can reduce this to average $SID_{QCCD} = 46(2.5)$, and average $SHD_{QCCD} = 15.1(1.6)$. In Table 4 we provide the average results over ten random sub-samples of the dataset where

the edges of CAM's CPDAG were oriented by each of the pairwise methods ⁶. From the presented results, we note that QCCD achieves best scores in terms of SHD and SID.

As such, it is reassuring that QCCD is able to correctly decide for the causal direction, even though other dependencies affect the pairwise (direct) causal relationships in such confounded dataset. While such results are promising, a consistent hybrid method extending QCCD to higher dimensional datasets is left for further work.

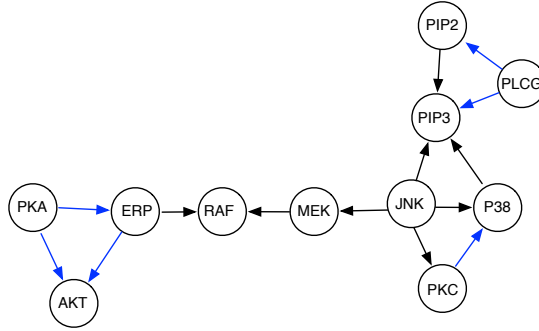


Figure 7: Causal protein network as obtained by CAM's CPDAG oriented with QCCD. Blue edges are correctly oriented.

Table 4: SID and SHD for the Sachs dataset using CAM CPDAG with causal directions from pairwise methods by 10-fold cross validation. Average and standard deviations.

	QCCD	IGCI-u	Slope	RESIT	CAM	EMD	LINGAM	GRAN	Random
SID	46.5(2.5)	50.3(1.9)	54.5(3.3)	51(0)	53.4(1.4)	51.5(2.7)	48.9(0.87)	49.5(4)	52.5(3.6)
SHD	15.1(1.6)	15.8(1.7)	17.6(1.2)	14(0.3)	15.4(1.6)	16(1.7)	14.3(0.82)	16.4(1.34)	17.2(1.4)

⁶We only included R based implementations.

E. Scatter plots of simulated pairs

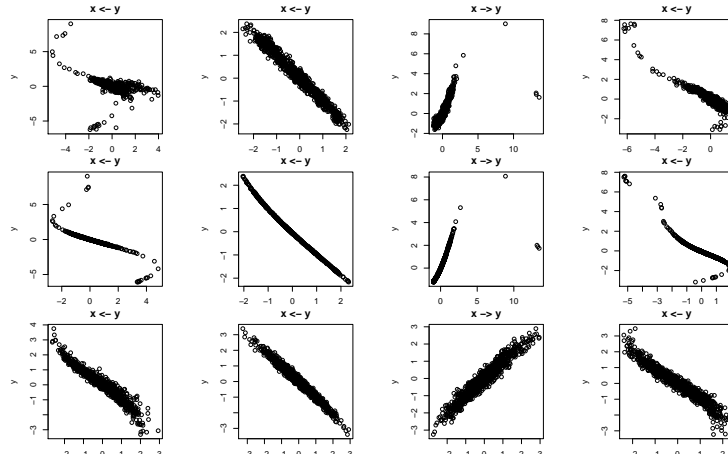


Figure 8: SIM/SIM-ln/SIM-G (first/second/third row).

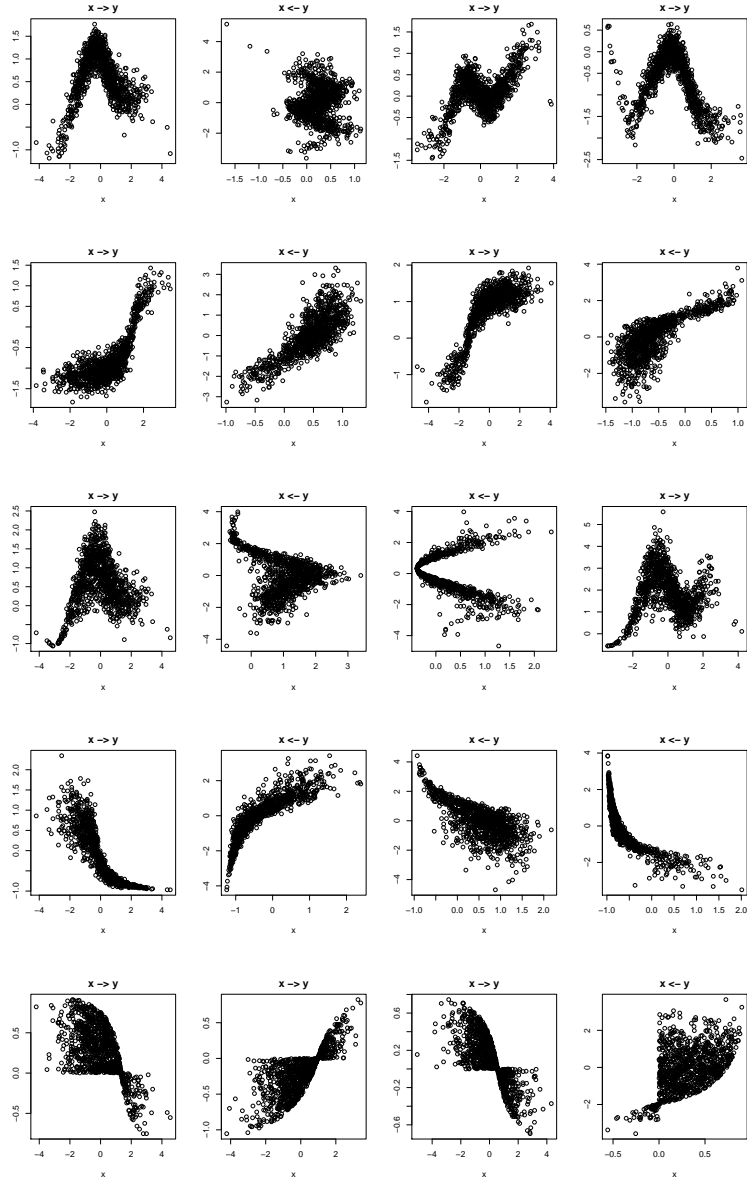


Figure 9: By row AN/AN-s/LS/LS-s/MN.

E.1. Computational complexity

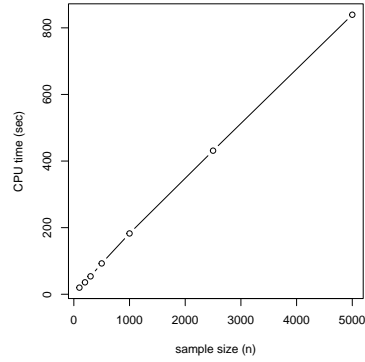


Figure 10: Linear scaling of QCCD over 100 pairs, $m = 1$, n varies.